Quaternary Science Reviews 150 (2016) 221–233

Contents lists available at ScienceDirect

Quaternary Science Reviews

journal homepage: www.elsevier.com/locate/quascirev

Differences between Last Glacial Maximum and present-day temperature and precipitation in southern South America

Ana Laura Berman [a], Gabriel E. Silvestri [a, *], Marcela S. Tonello [b]

[a] Centro de Investigaciones del Mar y la Atmósfera/CONICET-UBA, UMI IFAECI/CNRS, Int. Guiraldes 2160, Ciudad Universitaria, Buenos Aires, Argentina
[b] Laboratorio de Paleoecología y Palinología/Ecología y Paleoecología de Ambientes Acuáticos Continentales, Instituto de Investigaciones Marinas y Costeras (IIMyC), CONICET-UNMdP, J.B.Justo 2550, Mar del Plata, Argentina

ARTICLE INFO

Article history:
Received 15 June 2016
Received in revised form
15 August 2016
Accepted 16 August 2016

Keywords:
Last Glacial Maximum
South America
Pampa
Patagonia

ABSTRACT

This paper is the first analysis of differences between Last Glacial Maximum (LGM) and present climates in southern South America considering the state-of-the-art PMIP3 paleoclimatic models. The study is focused on characteristics of temperature and precipitation over the portion of the continent to the south of 20°S at both sides of the Andes Cordillera. Results demonstrate that model outputs coincide with glacial conditions inferred from the very few paleorecords available in the region. Consequently, these models are a valuable tool for inferring additional conditions in areas where there is a lack of proxy information allowing the reconstruction of the past climate at regional scales. The analyzed PMIP3 models expose an LGM cooling of ~2-5 °C throughout the year over almost all southern South America but differences are even more pronounced in areas around the southern Andes. Models also suggest that LGM precipitation was substantially lower than present over the portion of southern South America to the east of the Andes inferring reductions of ~20–30% with respect to present-day values in subtropical areas and ~40–50% in the southern tip of the continent.

1. Introduction

The Last Glacial Maximum (LGM; ~21,000 cal yr BP) is a significant period in the Earth's climate history. It was a time with atmospheric CO2 content about 50% of the present values, global mean temperature cooler than today and generalized expansion of ice sheets. Several studies have contributed to the knowledge of climate and environmental conditions on continents and oceans during the LGM that differ from those of the present in many aspects as land-sea distribution, ice cover, vegetation patterns, global winds, temperature and precipitation.

In South America, a review of estimated distribution of major environmental conditions and vegetation types during the LGM was made by Markgraf et al. (1992), Clapperton (1993), Adams and Faure (1997) and more recently by Marchant et al. (2009), among others. Inferences from different proxies suggest that the LGM was 5–10 °C cooler than present in tropical and subtropical areas of the continent (e.g., Farrera et al., 1999; Heine, 2000; Bush et al., 2001; Mayle et al., 2009 and references therein). Concerning moisture and precipitation conditions, paleoclimate information summarized by Vizy and Cook (2005) indicates that LGM was wetter than present in most sites located in tropical-subtropical Andes but drier than present in Amazonia and eastern Brazil. A drier LGM climate in the Amazonian rainforest and the Atlantic forest of Brazil would be consistent with the fact that precipitation over tropical South America is closely connected with moisture advection from the Atlantic Ocean. Consequently, cold conditions in surface waters (e.g., Niebler et al., 2003) can induce a reduction of moisture availability and precipitation over the continent. These results are in agreement with conclusions of model simulations performed by Cook and Vizy (2006) that indicate LGM annual mean precipitation over the Amazon basin 25–35% lower than present. This reduction is associated with a 2–3 month delay in the onset of the rainy season resulting in the glacial dry season to have been about twice as long as in present times. Moreover, results presented by Khodri et al. (2009) suggest the following conditions: i) LGM tropical dryness due to cooling effects was intensified by an equatorward shift of the northern boundary of the Hadley cell inducing subsidence over the area between 10°N and the equator; ii) dryness in

Abbreviations: EPat, Eastern Patagonia; LGM, Last Glacial Maximum; PMIP3, Paleoclimate Modelling Intercomparison Project Phase III; SACZ, South Atlantic convergence zone; SWP, Subtropical Wet Plain.

* Corresponding author.
E-mail addresses: alberman@cima.fcen.uba.ar (A.L. Berman), gabriel.emilio.silvestri@gmail.com (G.E. Silvestri), mtonello@mdp.edu.ar (M.S. Tonello).

http://dx.doi.org/10.1016/j.quascirev.2016.08.025
0277-3791/

the Amazon basin during the LGM was affected by a strengthening and eastward shift of the Walker circulation inducing an El-Niño like pattern over the region. In addition, Sylvestre (2009) reviewed LGM conditions inferred from sites located in tropical areas of South America concluding that there was enhanced aridity in the north of the continent while the moisture patterns exhibited distinct regional characteristics in the Amazon basin and wet conditions characterized the climate in Peruvian and Bolivian Andes. More details about climatic conditions during the LGM in South America, with emphasis in the area to the south of 20°S, are displayed in section 4.

Although global and regional characteristics of the LGM climate were analyzed considering different model simulations (e.g., Valdes, 2000; Wainer et al., 2005; Otto-Bliesner et al., 2006; Braconnot et al., 2007; Kim et al., 2008; Rojas et al., 2009; Braconnot et al., 2012; Kageyama et al., 2013), there is still a lack of studies of the glacial climate in southern South America considering both palaeoclimate proxy reconstructions and the state-of-the-art multimodel experiments from the Paleoclimate Modelling Intercomparison Project Phase III (PMIP3). In consequence, the objectives defined for this study are: (i) To perform a qualitative comparison of PMIP3 model outputs with a LGM multiproxy compilation in southern South America; (ii) To analyze characteristics of temperature and precipitation simulated by the models in order to obtain a more complete picture of the LGM climate in the region. Models can be especially useful to provide a realistic description of the past climate in areas where there is a lack of paleorecords and can also display characteristics of mean conditions during each season. These results will be an important contribution to the knowledge of time evolution of the regional climate that is valuable information for climate change scenarios associated with interactions between natural and anthropogenic forcings. It is important to mention that a detailed analysis of atmospheric anomalies responsible for changes detected in temperature and precipitation is beyond the scope of this study and will be examined in later publications.

The manuscript is organized as follows. Section 2 describes the study area, data and methodology. Section 3 shows observed and simulated characteristics of the present climate in South America. The comparison of paleoclimate models with proxy data and additional information provided by the models are discussed in section 4. Finally, conclusions are summarized in section 5.

2. Background information

2.1. Study area

The analysis is focused on the portion of South America to the south of 20°S comprising Argentina, Chile, Uruguay, Paraguay, southern Bolivia and southern Brazil. The area to the east of the Andes Cordillera is divided in three sub-regions (see inset in Fig. 1a) that are especially considered throughout the analysis: i) the subtropical wet plain (SWP) covering most of Paraguay, northeastern Argentina and part of southern Brazil; ii) the temperate Pampa extended over the centre of Argentina; iii) the arid eastern Patagonia (EPat) comprising the southeastern tip of the continent.

2.2. Data and methodology

2.2.1. Paleoclimate proxies

There are discrepancies about the timing of the LGM based on different terrestrial or oceanic records, and if LGM can be defined as a chronozone (e.g., Hughes and Gibbard, 2015). In this paper, the LGM is considered as the period between 18,000 and 24,000 cal yr BP following Mix et al. (2001). Consequently, a chronological control is applied to the paleorecords in order to obtain consistency and comparability of information that authors of each study assigned to the LGM. The criterion is to consider records of temperature and precipitation with at least one date in the interval 18,000–24,000 cal yr BP, independently of dating methods (radiocarbon or uranium/thorium). In cases of radiocarbon dates, we calibrate them using CALIB 7.0.0 with Southern Hemisphere curve (SHCal04) (McCormac et al., 2004; Stuiver et al., 2005) before applying the chronological control. Initially, a total of 43 sites were analyzed and just 24 sites fulfil the chronological criterion. Fig. 1 and Table 1 compile selected sites in the area where is focused this study. The corresponding characteristics are described in section 4.

2.2.2. PMIP3 models

The analysis is based on simulations of LGM and present climates performed with coupled ocean-atmosphere general circulation models included in the PMIP3 paleo-experiments that are part of the Coupled Model Intercomparison Project fifth phase (CMIP5). Although eight PMIP3 models simulate the glacial period, only four of them were selected for this study: models CCSM4, CNRM-CM5, MPI-ES-P and MRI-CGCM3 (see Table 2). The selection was made considering that these four models are able to reproduce the spatial distribution of present-day seasonal mean temperature and precipitation over the continent (see section 3) and differences between LGM and present-day climates inferred from the very few paleorecords available in the region (see section 4). Furthermore, these models are those with the highest spatial resolution (the highest density of grid points) which is important for describing climatic conditions in areas like southernmost South America where precipitation is strongly affected by the Andes Cordillera.

The imposed boundary conditions in LGM simulations are those inferred for 21,000 years ago (i.e., lower concentration in atmospheric greenhouse gases relative to present values, larger ice sheets in the Northern Hemisphere and orbital parameters nearly the same as present producing small differences in the insolation forcing). The present climate (PRES) is defined as the mean conditions during the modern period 1950–1999 obtained from the historical simulations of each model. Detailed descriptions of simulations and models can be found in Braconnot et al. (2012), Taylor et al. (2012) and the webpage of PMIP3 (http://pmip3.lsce.ipsl.fr).

The analysis is focused on annual and seasonal mean differences of temperature and precipitation simulated for past and present times by each individual model. The statistical significance of differences is assessed considering the Student's t-test (Brooks and Carruthers, 1953; Wilks, 2006). Austral seasons are considered as in the present: summer is December-January-February (DJF), autumn is March-April-May (MAM), winter is June-July-August (JJA) and spring is September-October-November (SON).

3. Present climate in South America

The present climate in South America has been extensively documented (e.g., Hoffman, 1975; Prohaska, 1976; Satyamurti et al., 1998; Garreaud et al., 2009). However, it is useful to provide a synthesis of the main features mentioned throughout this paper. The description is based on climatology (mean values in the period 1980–2010) of surface temperature extracted from the NCEP–NCAR reanalysis (Kalnay et al., 1996) and precipitation of the Climate Prediction Center Merged Analysis of Precipitation (CMAP; Xie and Arkin, 1997). The period 1980–2010 is selected because it includes satellite data, essential for the CMAP dataset and for a more precise description of the climate in the NCEP–NCAR reanalysis. Summer and winter mean conditions from these dataset and those of the present climate simulated for each PMIP3 model are shown in Figs. 2 and 3.

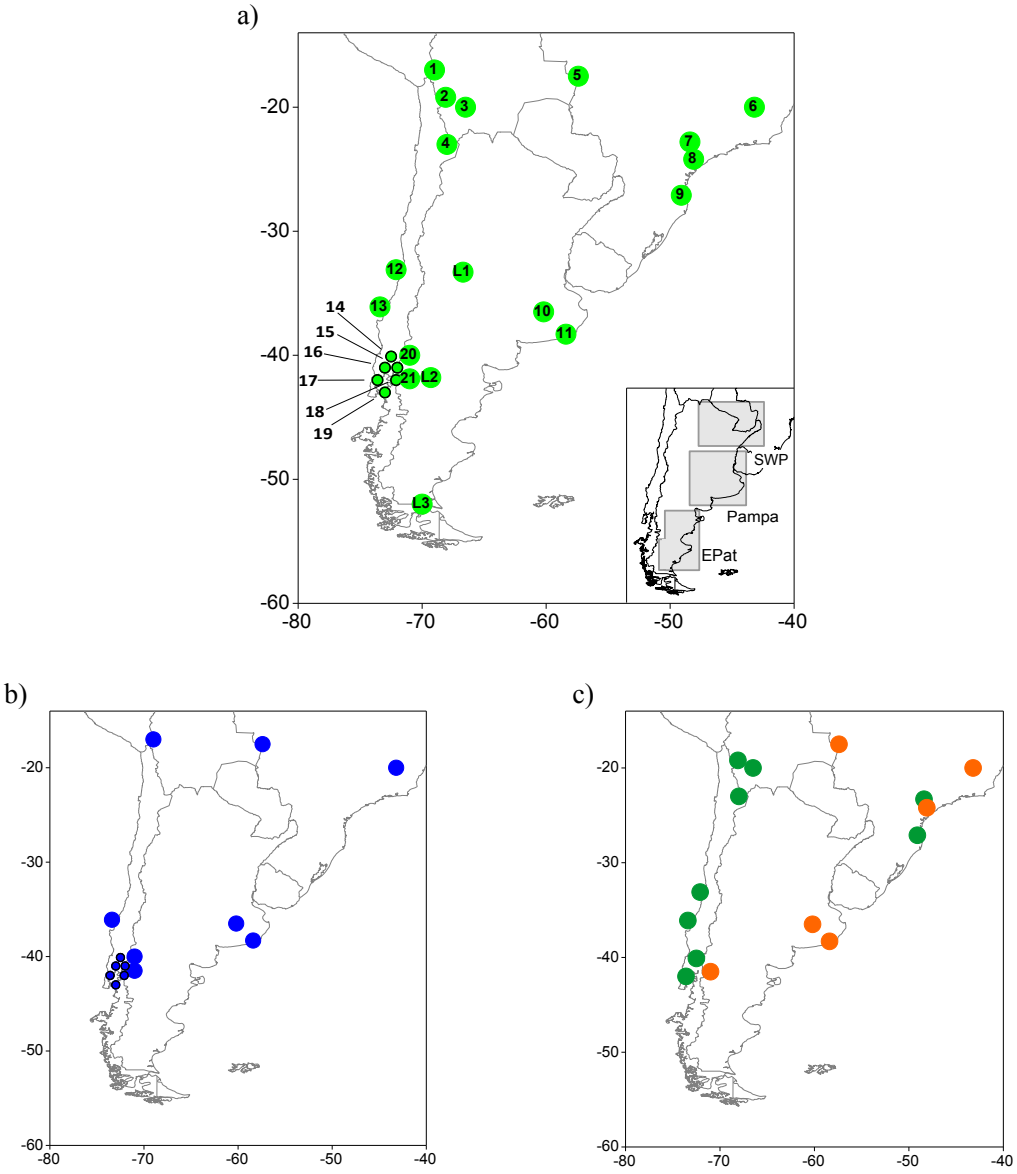

Fig. 1. a) Proxy data compilation for the LGM. See the corresponding references in Table 1. The circles associated with sites 14 to 19 are smaller due to graphical reasons. Shaded continental areas in the map of the right-bottom corner indicate the sub-regions Subtropical Wet Plain (SWP), Pampa and Eastern Patagonia (EPat) mentioned in the text. b) Reconstructed LGM temperature. Blue points (●) indicate LGM temperature lower than the present. c) Reconstructed LGM precipitation. Orange points (●) indicate LGM precipitation lower than the present and green points (●) indicate LGM precipitation higher than the present. (For interpretation of the references to colour in this figure legend, the reader is referred to the web version of this article.)

Continental surface temperature is affected by the elevation of topography and reduction of insolation with increasing latitude (Fig. 2a–b). Consequently, the spatial fields of near surface air temperature are characterized by an equator-to-pole reduction of seasonal mean values disturbed by asymmetries associated with the effect of the Andes Cordillera in the western portion of the continent. The north-south gradient of insolation also produces a marked annual cycle with warm summers and cold winters in extratropical latitudes. These characteristics are clearly detected in the three selected sub-regions (see observed conditions in Fig. 4a,b,c): seasonal mean temperatures reduce from SWP to EPat and summers are ~10 °C warmer than winters in the entire area.

Precipitation over tropical and subtropical continental areas exhibits a pronounced annual cycle with extreme phases in summer and winter (Fig. 3a–b) and the corresponding transitions during autumn and spring. The maximum of summer precipitation extends in a persistent northwest-southeast oriented band from the Amazon forest to the subtropical Atlantic Ocean that is known as the South Atlantic convergence zone (SACZ). The region of highest precipitation migrates northwestward during autumn and concentrates in the northern tip of the continent in winter when a dry season develops in most of the central portion of the continent. During spring, convection returns to the southeast and the intensification of the SACZ begins. To the south of 40°S, precipitation is strongly affected by the Andes Cordillera that intercepts the migratory synoptic systems embedded in the southern westerly flow producing abundant orographic precipitation and hyperhumid conditions around the mountains. In contrast, the westerly mean flow over the low-lying semi-arid steppe to the east of the southern Andes can be disturbed by strong synoptic episodes producing persistent easterly winds and advection of moisture from the South Atlantic that induce intense daily precipitation (Prohaska, 1976;

Table 1
Site name, proxy type, reconstructed variable(s) (T: temperature; Pr: precipitation), reconstructed season(s), chronological control (14C: number of radiocarbon dating and U/T: number of uranium/thorium dating in the interval 18,000–24,000 yr BP) and reference(s) of paleorecords considered in the study. The corresponding locations are indicated in Fig. 1. (*) Studies describing the "LGM climate" without mention to specific seasons are assumed as reconstructions of annual mean because annual mean represent mean conditions averaged over the entire period of time.

Site N°	Site name	Proxy type	Reconstructed variable(s)	Reconstructed season(s)	Chronological control		Reference(s)
					14C	U/T	
1	Lake Titicaca	pollen	T	annual *	3	0	Paduano et al. (2003)
2	Salar de Coipasa	diatom	Pr	annual *	5	0	Sylvestre (2002)
3	Salar de Uyuni	ionizing radiation	Pr	annual *	2	0	Baker et al. (2001)
4	Quebrada del Chaco	pollen	Pr	winter	4	0	Maldonado et al. (2005)
5	Laguna La Gaiba	pollen, diatom	Pr and T	annual *	3	0	Whitney et al. (2011)
6	Catas Altas	pollen	Pr and T	annual	1	0	Behling and Lichte (1997); Behling (2002)
7	Santana Cave	speleothem	Pr	annual *	0	2	Cruz et al. (2006); Cruz et al. (2007)
8	Parque Estadual Turístico Alto do Ribeira	pollen	Pr	annual *	1	0	Saia et al. (2008)
9	Botuverá Cave	speleothem	Pr	annual *	0	4	Cruz et al. (2005); Cruz et al. (2006); Cruz et al. (2007); Wang et al. (2007)
10	Salto de Piedra	mollusks	Pr and T	annual *	4	0	Bonadonna et al. (1999)
11	Paso Otero	mammal	Pr and T	annual *	3	0	Tonni et al. (1999)
12	Marine core GeoB 3302-1	terrigenous parameters	Pr	annual *	6	0	Lamy et al. (1999)
13	Marine core ODP 1234	pollen	Pr and T	annual, winter and summer	3	0	Lamy et al. (2004); Heusser et al. (2006)
14	Canal de la Puntilla	pollen	Pr and T	annual *	5	0	Moreno (1997); Moreno et al. (2015)
15	Lake Llanquihue	pollen	T	summer	7	0	Heusser et al. (2000)
16	Huelmo mire	chironomid	T	summer	2	0	Massaferro et al. (2014)
17	Chiloé Island	pollen	Pr and T	annual	2	0	Villagrán (1990)
18	Seno Reloncaví	pollen	T	summer	5	0	Denton et al. (1999); Heusser et al. (1999)
19	Corcovado-Chiloé	pollen	T	summer	8	0	Denton et al. (1999); Heusser et al. (1999)
20	Arroyo Corral Cave	mammal	T	annual *	3	0	Tammone et al. (2014)
21	Lake Mascardi	pollen	Pr and T	annual *	1	0	Bianchi and Ariztegui (2012)
L1	Salinas del Bebedero	dated beach ridges	lake level	annual *	2	0	Bradbury et al. (2001)
L2	Lake Cari Laufquen	dated shoreline stable isotopes	lake level	annual *	14	0	Galloway et al. (1988); Cartwright et al. (2011)
L3	Lake Potrok Aike	multiproxy	lake level	annual *	2	0	Kliem et al. (2013); Zolitschka et al. (2013)

Table 2
PMIP3 coupled ocean-atmosphere general circulation models employed in the study.

Model name	Atmosphere resolution (lon x lat)	LGM years simulated
CCSM4	1.25° × ~0.9°	100
CNRM-CM5	~1.4° × ~1.4°	200
MPI-ESM-P	~1.8° × ~1.8°	100
MRI-CGCM3	~1.12° × ~1.12°	100

Frumento, 2000; Mayr et al., 2007). The annual cycles of precipitation in sub-regions SWP and Pampa clearly display the subtropical pattern characterized by rainy summers and dry winters (see observed conditions in Fig. 4d–e) while the sub-region EPat exposes the reduction of precipitation throughout the year in the southern semi-arid steppe (Fig. 4f).

The above mentioned characteristics of the spatial structure of seasonal mean fields of temperature and precipitation over South America are correctly reproduced by the four PMIP3 models selected for this study, although inter-model differences are detected in the corresponding seasonal mean values (see Figs. 2–4). Models abilities to reproduce the spatial distribution of seasonal mean temperature and precipitation over South America, inter-model differences and differences between models and observations are coincident with conclusions of several previous studies focused on different global and/or regional simulations. Among others, Vera et al. (2006) showed that global models are able to reproduce the main features of the seasonal cycle of present-day precipitation over South America but there are large discrepancies in the corresponding mean magnitudes. Silvestri et al. (2009), Carril et al. (2012) and Solman et al. (2013) demonstrated that regional models have reasonable skill in representing the spatial distribution of present-day seasonal temperature and precipitation in South America but they have some deficiencies in reproducing accurately the observed mean values.

4. LGM climate

4.1. Paleoclimate proxies

Fig. 1 summarizes the selected sites and reconstructed changes between LGM and present-day temperature and precipitation based on inferences from paleoclimatic proxies. These changes are synthesized in the following paragraphs.

In areas of the southern Bolivian Altiplano, reconstructed vegetation history of Lake Titicaca (site 1) indicates that very cold climatic conditions prevailed during the LGM, with temperatures suggested to be at least 5–8 °C cooler than present (Paduano et al., 2003). Moreover, a high-resolution diatom study in Salar de

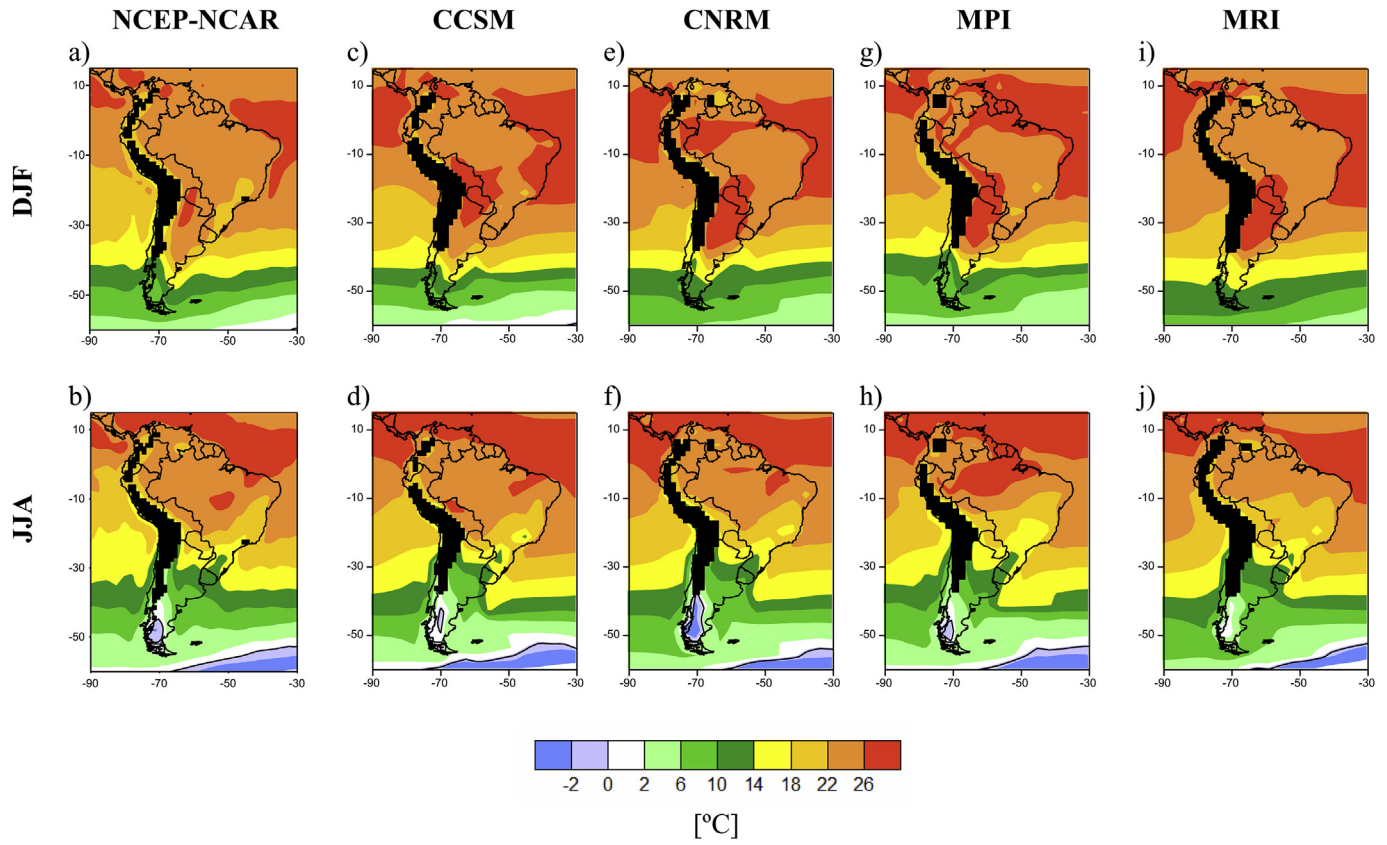

Fig. 2. Summer and winter mean surface temperature (°C) for NCEP-NCAR reanalysis in 1980–2010 and each PMIP3 model in 1950–1999. Black areas indicate topography higher than 1200 m.

Coipasa (site 2) suggests that this basin was filled by a shallow salt lake during the LGM implying climatic conditions more humid than present (Sylvestre, 2002). Coherently, natural g-rays measures on sediment cores of Salar de Uyuni (site 3) indicate that LGM precipitation was 30% higher than present (Baker et al., 2001) and pollen series of Quebrada del Chaco (Atacama Desert, site 4) suggest winter precipitation higher than today (Maldonado et al., 2005).

Pollen and diatoms records from Laguna La Gaiba (site 5) located in areas of the Pantanal, the largest tropical wetland of the world, suggests that the LGM climate was drier and colder than today in these interior lowlands (Whitney et al., 2011).

In southeastern Brazil, pollen records from the area of Catas Altas (site 6) suggest that the LGM climate was markedly drier than today and annual mean temperature was at least 5-7 °C lower than the present values (Behling and Lichte, 1997; Behling, 2002). A study of vegetation dynamics in forest ecosystems of Parque Alto do Ribeira (site 8) also suggests that the glacial climate was drier than present (Saia et al., 2008). In contrast, speleothem collected in Santana and Botuverá caves (sites 7 and 9) indicate that the LGM climate was wetter than today (Cruz et al., 2005, 2006, 2007; Wang et al., 2007). These discrepancies could be related to multiple factors influencing the relationships between proxies considered in each study and local environmental conditions.

In southern Pampa (sites 10 and 11), predominance of arid climates during the LGM, with temperature and precipitation lower than those of present times, are inferred from mammal and mollusks records (Bonadonna et al., 1999; Tonni et al., 1999; and references therein).

To the west of the Andes Cordillera, terrigenous sediment parameters on marine cores from the continental slope off central Chile (site 12) suggest that the LGM climate was wetter than present (Lamy et al., 1999). Pollen records from marine sediments near central Chile (site 13) indicate glacial annual precipitation ~2000 mm higher than present while winter and summer temperatures could be ~5 °C and ~3 °C lower, respectively (Lamy et al., 2004; Heusser et al., 2006). Southward, pollen records from Canal de la Puntilla (site 14) suggest that the LGM climate was colder and wetter than present (Moreno, 1997; Moreno et al., 2015). In addition, characteristics of the reconstructed vegetation from Chiloé Island (site 17) implies a decrease in annual mean temperature of at least 4 °C and an increase in annual precipitation of at least 1500 mm during the LGM with respect to present conditions (Villagrán, 1990; and references therein). Furthermore, pollen records from Lake Llanquihue (site 15), Seno Reloncaví (site 18) and Corcovado-Chiloé (site 19) suggest that LGM summer temperatures were 6-8 °C below present values (Denton et al., 1999; Heusser et al., 1999, 2000) and a quantitative reconstruction based on the chironomid record of the Huelmo mire (site 16) indicate that LGM mean temperature of the three warmest months was 2–4 °C lower than modern values (Massaferro et al., 2014).

In areas of Patagonia to the east of the Andes Cordillera, analyses of small mammal assemblages from the archeological cave Arroyo Corral (site 20) indicate that, in general, LGM habitats appear to be more open, barren and colder than today (Tammone et al., 2014). In addition, pollen records from Lake Mascardi (site 21) suggest that the regional LGM climate was drier and probably colder than today (Bianchi and Ariztegui, 2012). Although there is a lack of paleoclimate records for the LGM in southern Patagonia that fulfil the chronological control, several pollen data agree that glacial influence ceased at ~17,000 cal yrs BP (e.g., Markgraf and Huber, 2010;

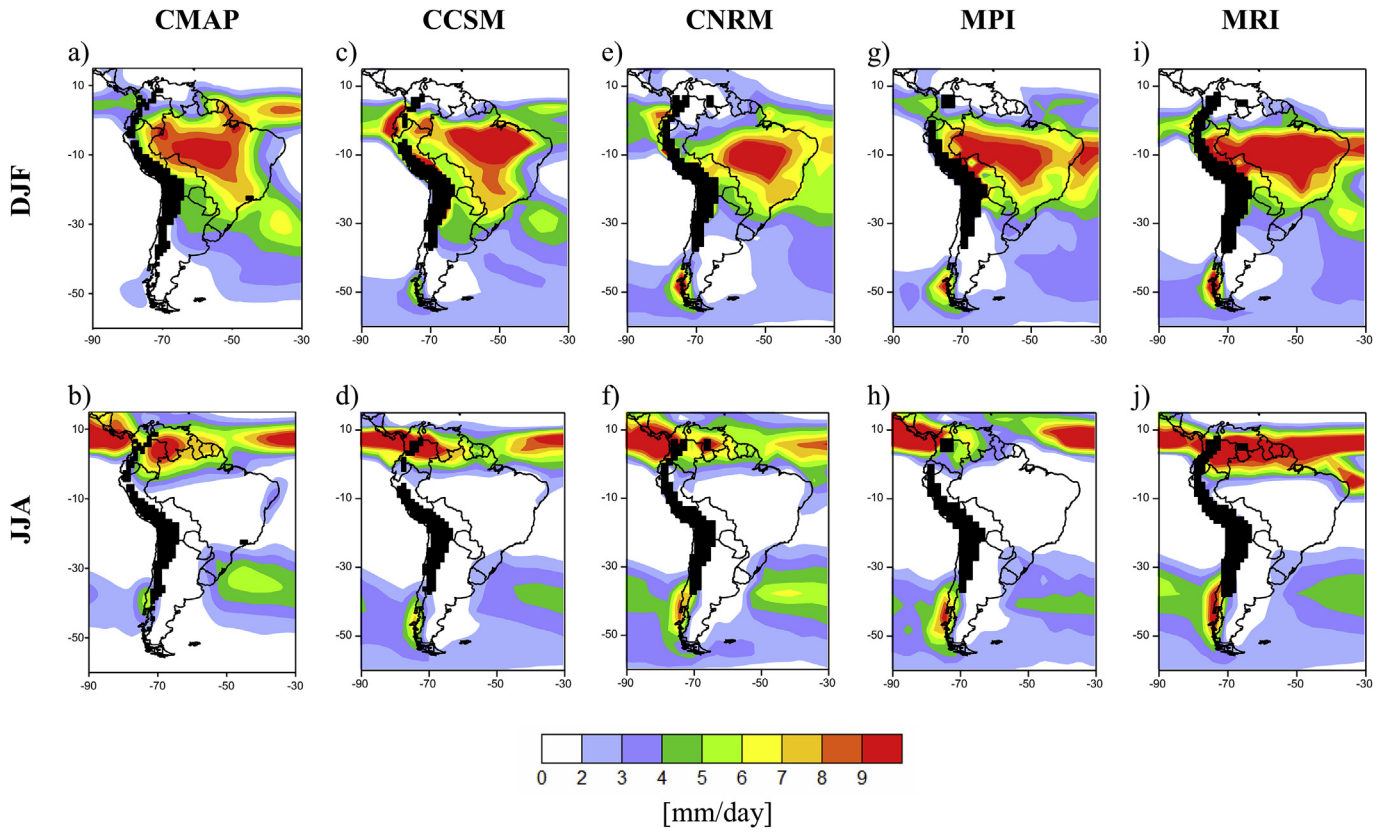

Fig. 3. Summer and winter mean precipitation (mm/day) for CMAP in 1980–2010 and each PMIP3 model in 1950–1999. Black areas indicate topography higher than 1200 m.

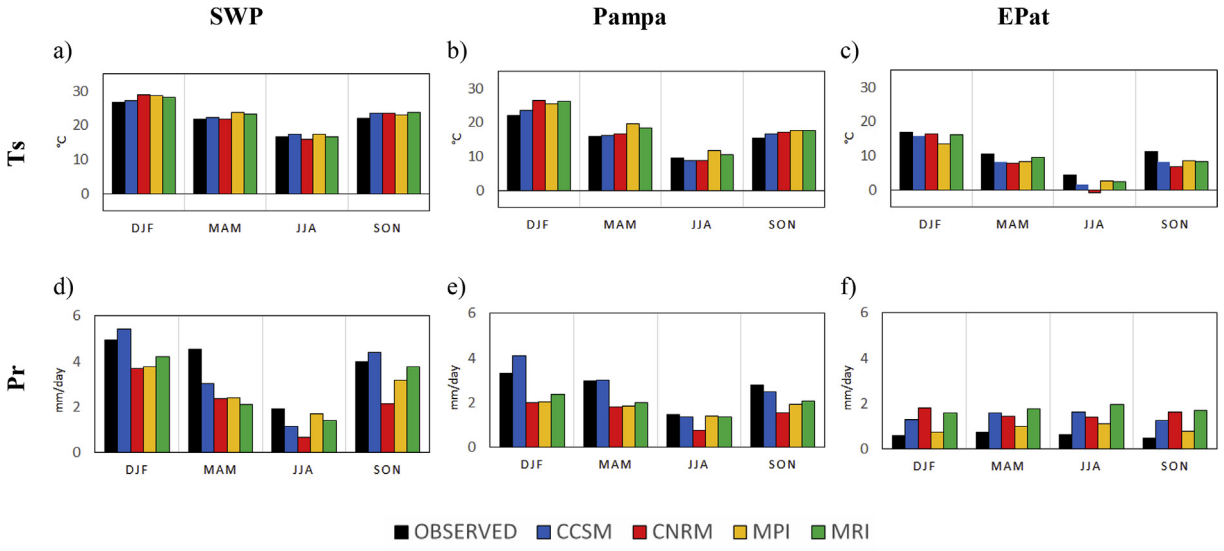

Fig. 4. Observed and simulated seasonal mean surface temperature (Ts) and precipitation (Pr) during 1950–1999 in the sub-regions SWP; Pampa and EPat. Observed values were taken from meteorological stations of the GHCN dataset (see Supplementary Fig. S1).

Fontana and Bennett, 2012) and model simulations suggested a slow rate of deglaciation in the southern sector of the Patagonian ice sheet associated with a warming pulse (Hulton et al., 2002).

Reliable information of glacial times can be found in two lakes located in western Argentina. In fact, paleolimnological data indicate that the LGM lake-level stage at Salinas del Bebedero (site L1) was ~20–25 m above the present-day playa surface (Bradbury et al., 2001; and references therein) and reconstructions of Lake Cari Laufquen (site L2) suggest that the LGM level was ~25–40 m higher than present (Galloway et al., 1988; Cartwright et al., 2011). This information has to be considered with caution because both lakes respond to precipitation and snowmelt over the Andes Cordillera and might not represent characteristics of local changes in precipitation and/or temperature. In consequence, both sites are excluded from Fig. 1b–c.

Several studies demonstrated that Patagonian glaciers and ice

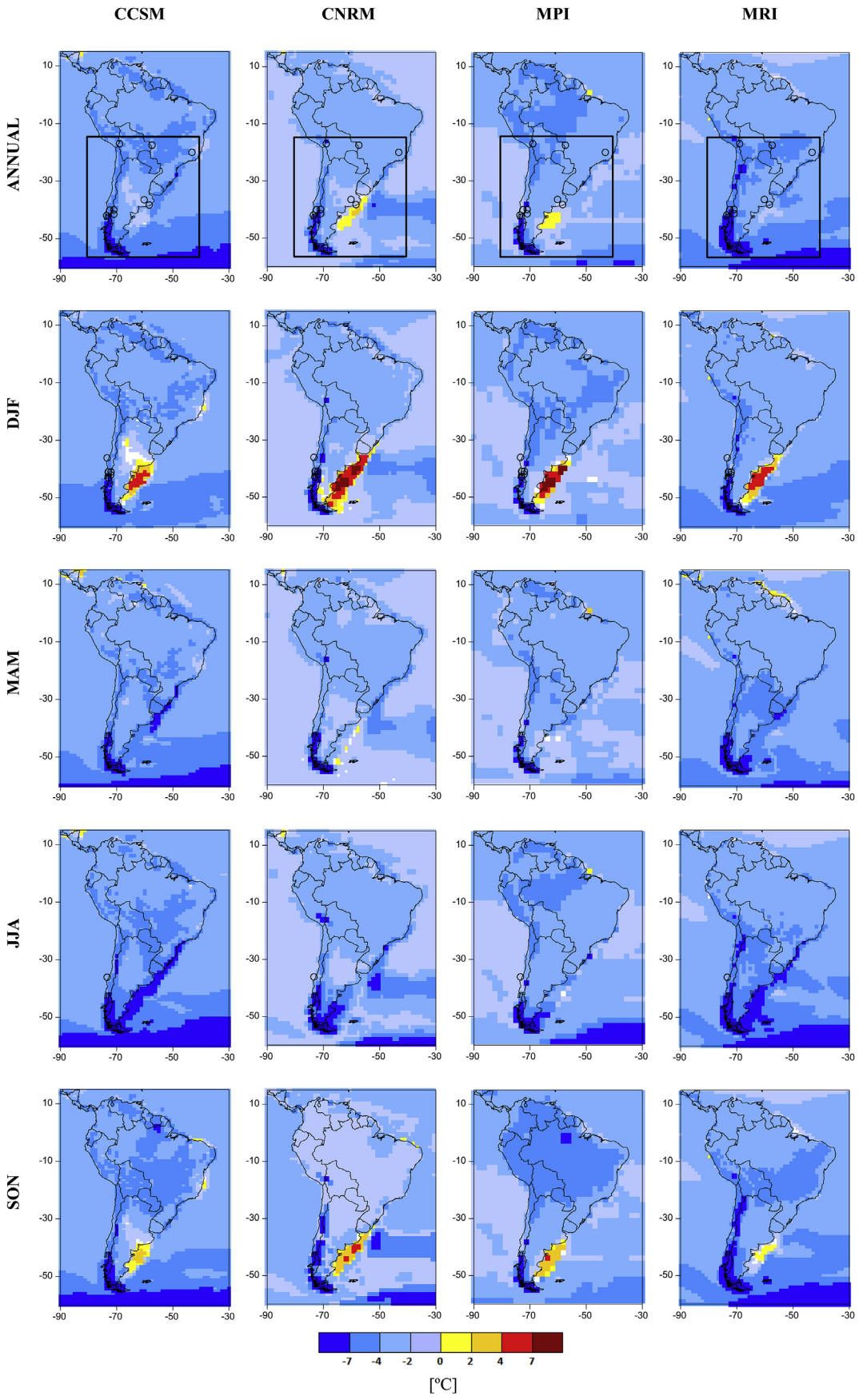

Fig. 5. Differences LGM minus present for annual and seasonal mean surface temperature simulated by each PMIP3 model. Differences are significant at 95% in all grid points except in the few ones in white. Empty circles indicate sites where LGM temperature was lower than the present (see Fig. 1b and Table 1). Black squares in maps of annual differences delimit the continental area of Fig. 1.

sheet expanded into the lowlands on both sides of the Andes during the LGM (e.g., Rabassa and Clapperton, 1990; Hulton et al., 2002; Heusser, 2003; Sagredo et al., 2011; Ponce and Fernández, 2014). In this context, reconstructions of Lake Potrok Aike (site L3) indicate that the level during the LGM was almost 20 m above the present values (Kliem et al., 2013; Zolitschka et al., 2013; and references therein). Kliem et al. (2013) argued that permafrost during the LGM might have enforced superficial runoff and caused higher levels in Potrok Aike. In other words, high lake levels during the glacial period are not necessarily related to increased precipitation or decreased evaporation in the area. Accordingly, this site is excluded from Fig. 1b–c.

4.2. PMIP3 models

Differences between LGM and present-day temperature and precipitation simulated by each model are shown in Figs. 5 and 7, respectively, while differences for the mean values in sub-regions SWP, Pampa and EPat are displayed in Fig. 8. The main aspects of these annual and seasonal characteristics can be synthesized as follows.

4.2.1. Temperature

The spatial structure of the seasonal mean fields of temperature during the LGM are similar to those of present in the four models (figures not shown) but the corresponding mean values are significantly different. In general terms, continental areas indicate overall annual and seasonal LGM cooling with magnitudes not spatially uniform (Fig. 5). Meridional cross sections of present-day temperature over tropical-subtropical continental areas (Fig. 6) show small latitudinal differences in summer and marked north-south gradient in winter as consequence of the annual cycle of insolation. The four models suggest that these continental thermal profiles had the same structure during the LGM but magnitudes were lower than present in all latitudes. The simulated continental cooling agrees with the general condition inferred from paleoclimatic proxies synthesized in the previous section indicating that the four models can provide a realistic picture of the past temperature in the entire region.

Modeled annual mean differences show a continental glacial cooling of ~2-4 °C with respect to the present values in the four models. Although the analysis of past conditions in the ocean is not the aim of this study, it is important to mention that the four models are also able to reproduce the glacial annual cooling in tropical-subtropical areas of the South Atlantic inferred by Niebler et al. (2003), among others.

In summer, models suggest a statistically significant LGM cooling of ~1-5 °C over the continent but differences are even more pronounced in areas around the southern Andes. Magnitudes of differences in the three selected sub-regions differ among models being of ~2-4 °C in SWP, ~1-2.5 °C in Pampa and ~1–2.7 in EPat (Fig. 8a,b,c). In contrast to these LGM cooling over the continent, significant warming of more than 3 °C is inferred in the South-western Atlantic near the continent (Fig. 5) where the sea level was markedly lower during glacial times. In fact, Ponce et al. (2011) reconstructed the palaeogeographical evolution of the continental shelf in Patagonia during the LGM estimating that the eastern boundary of the continental area extended approximately 450 km farther east from its present location as a consequence of the global fall of sea levels. In other words, a large portion of the present submerged Argentine Continental Shelf was exposed developing an enormous plain along the Atlantic coast during glacial times. Consequently, summer insolation heated these areas and PMIP3 models suggest that the corresponding surface temperature was warmer than the superficial cold waters that cover the region in the present.

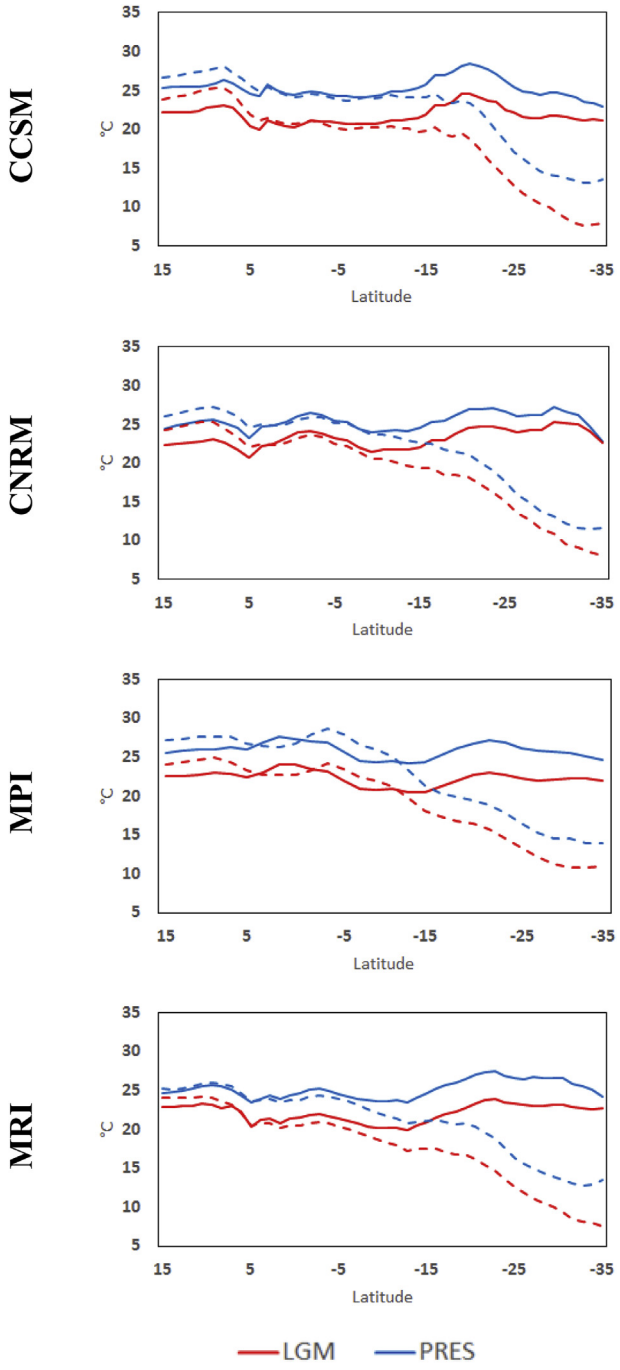

Fig. 6. Meridional cross section of summer (solid lines) and winter (dashed lines) mean temperature in the band 50°-62°W simulated by each PMIP3 model for LGM (red) and present (blue) times. (For interpretation of the references to colour in this figure legend, the reader is referred to the web version of this article.)

Significant LGM cooling over the whole continent persists during autumn with differences of ~2.5–4.2 °C in SWP, ~1.5–4.2 °C in Pampa and ~2-4.3 °C in EPat (Fig. 8a,b,c). Coinciding with the reduction of insolation during these months in middle latitudes due to the annual cycle of incoming solar radiation, the anomalous warming in the Argentine Continental Shelf detected in summer gradually reduces being replaced by colder LGM temperatures (Fig. 5).

In winter, cold conditions during the LGM were more

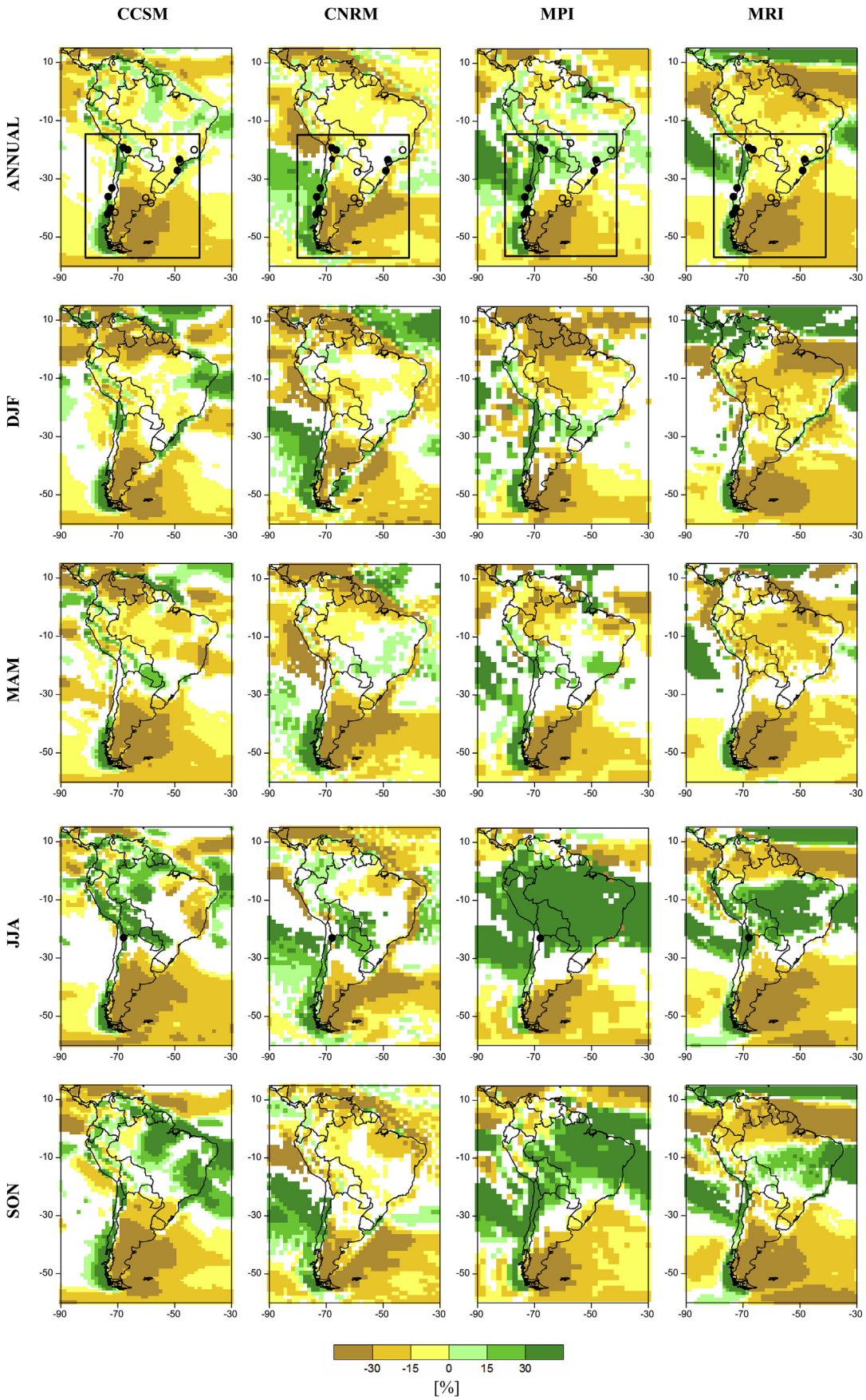

Fig. 7. Differences LGM minus present for annual and seasonal mean precipitation simulated by each PMIP3 model. Only differences significant at 95% are shown and values are in percentage of present (PRES) mean precipitation (i.e., difference=(LGM-PRES)x100/PRES). Empty (filled) circles indicate sites where LGM precipitation was lower (higher) than the present (see Fig. 1c and Table 1). Black squares in maps of annual differences delimit the continental area of Fig. 1.

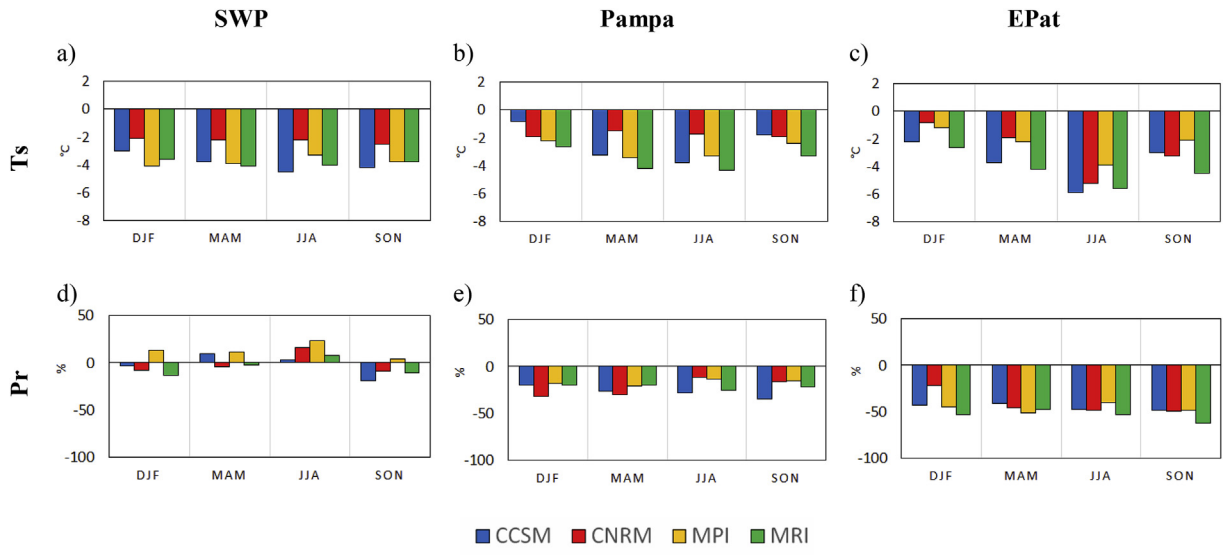

Fig. 8. Differences LGM minus present for seasonal mean surface temperature (Ts) and precipitation (Pr) simulated by each PMIP3 model in the sub-regions SWP, Pampa and EPat. Differences of precipitation are in percentage of present (PRES) mean values (i.e., difference=(LGM-PRES)x100/PRES).

pronounced with cooling of ~2.5–4.5 °C in SWP, ~1.7–4.3 °C in Pampa and ~3.9–5.9 °C in EPat (Fig. 8a-b-c) but differences of ~8 °C are detected in the four models around the southernmost Andes (Fig. 5). Models also display a pronounced cooling in areas of the Argentine Continental Shelf that were exposed during the LGM. The reduction of winter insolation in middle latitudes due to the annual cycle of incoming solar radiation induces low continental temperatures and can explain that the glacial surface temperatures over these areas were colder than those of the present-day superficial waters.

Spring represents a transition from the conditions observed in winter to those of summer. The pronounced LGM continental cooling detected in winter gradually reduces and warmer conditions over the Argentine Continental Shelf begin as a consequence of increased insolation due to its annual cycle. The simulated glacial cooling is ~2.5–4.2 °C in SWP, ~1.8–3.3 °C in Pampa and ~2.1–4.5 °C in EPat (Fig. 8a-b-c).

Figures 5 and 8a-b-c expose inter-model differences in the magnitude of temperature changes simulated for southern South America. However, there is total coherence in the sign of the climate change because the four models describe a glacial climate colder than today in the four seasons.

4.2.2. Precipitation

Although the spatial structure of the seasonal mean fields of LGM precipitation reproduced by each model are similar to those of the present-day described in section 3 (figures not shown), the corresponding mean values are significantly different over broad areas of South America including the southern portion of the continent that is the focus of this paper (Figs. 7 and 8d-e-f). Significant differences of annual mean precipitation over southern continental areas show two characteristics detected in the four models that are coincident with those inferred from the available paleoclimatic proxies: i) LGM precipitation was lower than present in the region to the south of 30°S and to the east of the Andes Cordillera; ii) LGM precipitation was higher than present over southern Chile (the western portion of the continent to the south of 35°S and to the west of the Andes). In contrast, discrepancies among models are detected in the sign of the change over the central and northern portions of the continent.

To the north of 20°S, models indicate statistically significant reduction of summer precipitation during the LGM with respect to the present values. A glacial climate drier than today in tropical-subtropical South America during summer is consistent with cold sea surface waters in the tropical Atlantic and the consequent reduction of moisture advection from the ocean to the continent (see characteristics of present-day water vapor flux over South America in Berbery and Collini, 2000; Arraut and Satyamurty, 2009). Dryness over those areas can be also associated with weakened convection due to colder LGM continental temperatures. In fact, the four models display that the meridional cross section of summer precipitation over tropical-subtropical continental areas has the same structure in both periods but magnitudes were clearly lower during the LGM (Fig. 9). This feature might indicate that past and present deep convection associated with the SACZ develops over similar areas but the corresponding intensity was significantly lower during glacial times. However, further analyses of the SACZ dynamics during the LGM must be done in order to confirm this hypothesis. In contrast to the summer conditions, marked discrepancies among models in the sign and magnitude of the change are detected in central and northern South America in autumn, winter and spring. This lack of agreement among models could be associated with discrepancies in the representation of changes in dynamical conditions influencing regional precipitation but such analysis is beyond the scope of this paper.

To the south of 20°S, discrepancies among models like those mentioned in the previous paragraph are detected in the sub-region SWP (Fig. 8d). In contrast, the four models agree in simulate a reduction of LGM precipitation with respect to the present values over a wide area to the east of the Andes that include the sub-regions Pampa and EPat (reductions of ~20–30% and ~40–50%, respectively; Fig. 8e–f) while increased precipitation is modeled over southern Chile (Fig. 7). These conditions detected throughout the year can be associated with different processes. In fact, LGM climate drier than present in the sub-region Pampa is consistent with reduced moisture content in the Amazon that, in turn, induces reduced moisture advection to subtropical regions. At higher latitudes, cold sea waters in the Southwestern Atlantic during the LGM could reduce the advection of moisture from the ocean to EPat inducing regional dryness during glacial times. Furthermore, precipitation associated with frontal systems that penetrate both

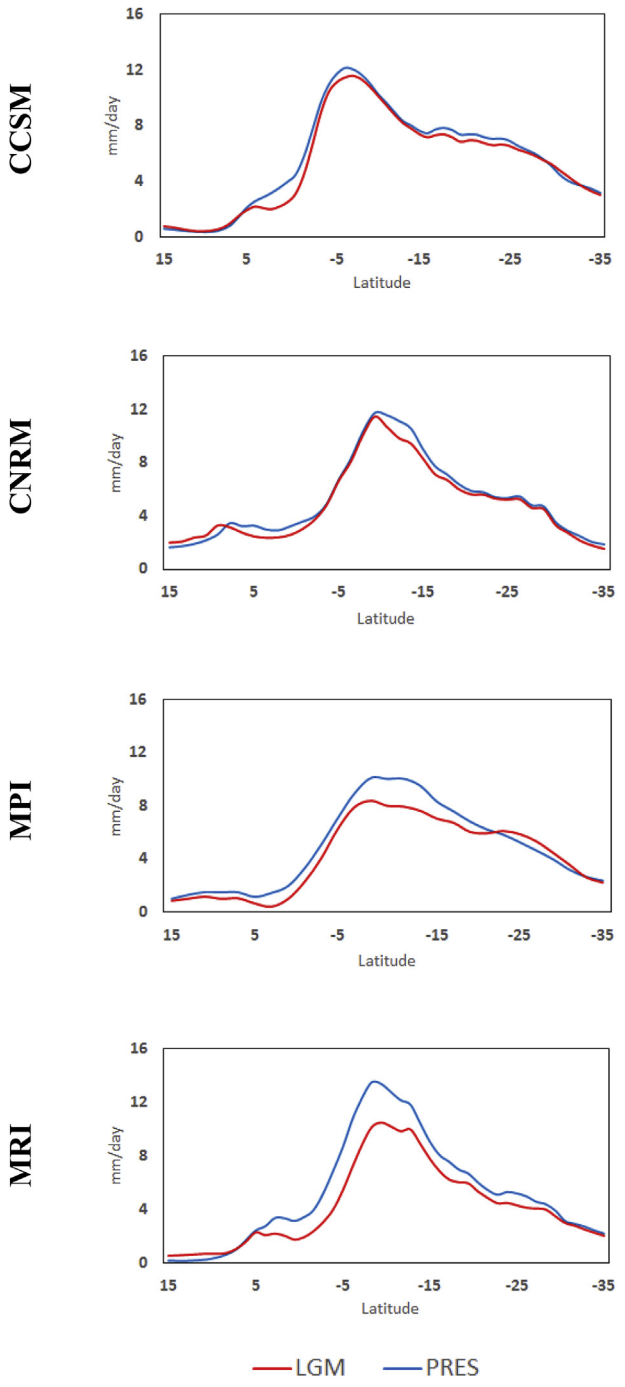

Fig. 9. Meridional cross section of summer mean precipitation in the band 50°-62°W simulated by each PMIP3 model for LGM (red) and present (blue) times. (For interpretation of the references to colour in this figure legend, the reader is referred to the web version of this article.)

Pampa and EPat from the south could be reduced during the LGM due to extremely cold and dry conditions of polar air masses. On the other hand, increased LGM precipitation around the southern Andes could indicate changes in characteristics of the southern storm tracks and/or the westerly winds over the region. However, it is important to take into account that the intensity and latitudinal position of the maximum southern westerlies is an aspect of the glacial climate with ambiguous results and permanent debate (e.g., Rojas et al., 2009; Kohfeld et al., 2013; Rojas, 2013; Sime et al., 2013; and references therein).

5. Conclusions

Several initiatives and working groups pointed out the need to analyze paleoclimatic proxies jointly with model simulations in order to understand climate changes in response to natural and anthropogenic forcings. In this context, the analysis developed here constitutes a pioneering study of differences between LGM and present-day climates in southern South America simulated by the state-of-the-art PMIP3 paleoclimatic models. The objective is to infer characteristics of glacial temperature and precipitation that complement those conditions extracted from the very few paleorecords available in the region. Models are used to provide valuable description of annual and seasonal past conditions in areas where there is a lack of proxy information allowing the reconstruction of the glacial climate at regional scales. Consequently, this study shows a complete picture of temperature and precipitation in southern South America during the LGM. In addition, the proxy compilation allows the identification of key areas where new adequate paleorecords, in terms of proxy-sensitive and good resolution time, should be requested to the paleoclimate community.

Past conditions inferred from proxies suggest that LGM temperature was significantly lower than present in southern South America. The analyzed PMIP3 models reproduce this general condition and expose an overall LGM cooling of ~1-5 °C throughout the year over the region with the most pronounced differences (glacial cooling of ~8 °C) over areas of southern Patagonia in winter.

The selected PMIP3 models agree with the available proxies in describing LGM precipitation substantially lower than present over the southern portion of the continent to the east of the Andes Cordillera and precipitation higher than present over central-southern Chile. Models suggest a reduction of ~20–30% with respect to present-day values in seasonal precipitation over Pampa and ~40–50% over eastern Patagonia.

The analysis of atmospheric anomalies responsible for changes detected in regional precipitation is beyond the scope of this study. This issue will be treated in companion papers that will be focused on the analysis of the following aspects of the LGM climate in South America: i) moisture transport from tropical areas to the subtropical plains and Pampa; ii) moisture advection from the Southwestern Atlantic to eastern Patagonia; iii) intensity and annual cycle of the southern westerlies over Patagonia. Studies as those performed by Berbery and Collini (2000) and Arraut and Satyamurty (2009) provide guidelines for improving the knowledge of the atmospheric circulation and water vapor flux over South America during glacial times.

Acknowledgements

Authors acknowledge the climate modelling groups (listed in Section 2) for producing and making available their model output. Comments and suggestions provided by Vera Markgraf and an anonymous reviewer were very helpful in improving this paper. Ana Laura Berman and Gabriel Silvestri were financed by Grants CONICET-PIP 11220120100526CO and AGENCIA-MINCYT-PICT-2013-0043. Marcela Tonello acknowledges support from Grants UNMdP EXA 807/16 and EXA 775/16.

Appendix A. Supplementary data

Supplementary data related to this article can be found at http://dx.doi.org/10.1016/j.quascirev.2016.08.025.

References

Adams, J., Faure, H., 1997. Preliminary vegetation maps of the world since the Last

Glacial Maximum: an aid to archaeological understanding. J. Archaeol. Sci. 24, 623–647.
Arraut, J.M., Satyamurty, P., 2009. Precipitation and water vapor transport in the Southern Hemisphere with emphasis on the South American region. J. Appl. Meteor. Climatol. 48, 1902–1912.
Baker, P.A., Rigsby, C.A., Seltzer, G.O., Fritz, S.C., Lowenstein, T.K., Bacher, N.P., Veliz, C., 2001. Tropical climate changes at millennial and orbital timescales on the Bolivian Altiplano. Nature 409, 698–701.
Behling, H., Lichte, M., 1997. Evidence of dry and cold climatic conditions at glacial times in tropical southeastern Brazil. Quat. Res. 48, 348–358.
Behling, H., 2002. South and southeast Brazilian grasslands during Late Quaternary times: a synthesis. Palaeogeogr. Palaeoclimatol. Palaeoecol. 177, 19–27.
Berbery, E.H., Collini, E.A., 2000. Springtime precipitation and water vapor flux over Southeastern South America. Mon. Wea. Rev. 128, 1328–1346.
Bianchi, M., Ariztegui, D., 2012. Vegetation history of the Río Manso Superior catchment area, Northern Patagonia (Argentina), since the last deglaciation. Holocene 22 (11), 1283–1295.
Bonadonna, F., Leone, G., Zanchetta, G., 1999. Stable isotope analyses on the last 30 ka molluscan fauna from Pampa grassland, Bonaerense region, Argentina. Palaeogeogr. Palaeoclimatol. Palaeoecol. 153, 289–308.
Braconnot, P., Otto-Bliesner, B., Harrison, S., Joussaume, S., Peterchmitt, J.-Y., Abe-Ouchi, A., Crucifix, M., Driesschaert, E., Fichefet, Th, Hewitt, C.D., Kageyama, M., Kitoh, A., Laîné, A., Loutre, M.-F., Marti, O., Merkel, U., Ramstein, G., Valdes, P., Weber, S.L., Yu, Y., Zhao, Y., 2007. Results of PMIP2 coupled simulations of the Mid-Holocene and Last Glacial Maximum-part 1: experiments and large scale features. Clim. Past. 3, 261–277.
Braconnot, P., Harrison, S.P., Kageyama, M., Bartlein, P.J., Masson-Delmotte, V., Abe-Ouchi, A., Otto-Bliesner, B., Zhao, Y., 2012. Evaluation of climate models using palaeoclimatic data. Nat. Clim. Change 2, 417–424. http://dx.doi.org/10.1038/nclimate1456.
Bradbury, J., Grosjean, M., Stine, S., Sylvestre, F., 2001. Full and Late Glacial lake records along the PEP1 transect: their role in developing interhemispheric paleoclimate interactions. In: Markgraf, V. (Ed.), Interhemispheric Climate Linkages; Present and Past Interhemispheric Climate Linkages in the Americas and their Societal Effects. Academic Press, New York, pp. 265–291.
Brooks, C., Carruthers, N., 1953. Handbook of Statistical Methods in Meteorology. Her Majesty's Stationery Office, London.
Bush, M., Stute, M., Ledru, M.-P., Behling, H., Colinvaux, P.A., de Oliveira, P.E., Grimm, E.C., Hooghiemstra, H., Haberle, S., Leyden, B.W., Salgado-Labouriau, M.-L., Webb, R., 2001. Paleotemperature estimates for the lowland americas between 30°S and 30°N at the Last Glacial Maximum. In: Markgraf, V. (Ed.), Interhemispheric Climate Linkages; Present and Past Interhemispheric Climate Linkages in the Americas and their Societal Effects. Academic Press, Elsevier, New York, pp. 293–306.
Carril, A.F., Menéndez, C.G., Remedio, A.R., Robledo, F., Sorensson, A., Tencer, B., Boulanger, J.-P., de Castro, M., Jacob, D., Le Treut, H., Li, L.Z., Penalba, O., Pfeifer, S., Rusticucci, M., Salio, P., Samuelsson, P., Sanchez, E., Zaninelli, P., 2012. Performance of a multi-RCM ensemble for south Eastern South America. Clim. Dyn. 39, 2747–2768.
Cartwright, A., Quade, J., Stine, S., Adams, K., Broecker, W., Cheng, H., 2011. Chronostratigraphy and lake-level changes of Laguna Cari-Laufquén, Río Negro, Argentina. Quat. Res. 730, 430–440.
Clapperton, C.M., 1993. Nature of environmental changes in south America at the last glacial maximum. Palaeogeogr. Palaeoclimatol. Palaeoecol. 101, 189–208.
Cook, K.H., Vizy, E.K., 2006. South american climate during the last glacial maximum: delayed onset of the south american monsoon. J. Geophys. Res. 111, D02110. http://dx.doi.org/10.1029/2005JD005980.
Cruz, F., Burns, S.J., Karmann, I., Sharp, W.D., Vuille, M., Cardoso, A.O., Ferrari, J.A., Silva Dias, P.L., Viana Jr., O., 2005. Insolation-driven changes in atmospheric circulation over the past 116,000 years in subtropical Brazil. Nature 434, 63–66.
Cruz, F., Burns, S., Karmann, I., Sharp, W., Vuille, M., 2006. Reconstruction of regional atmospheric circulation features during the Late Pleistocene in subtropical Brazil from oxygen isotope composition of speleothems. Earth Planet. Sci. Lett. 248 (1), 495–507.
Cruz, F., Burns, S.J., Jercinovic, M., Sharp, W.D., Karmann, I., Vuille, M., 2007. Evidence of rainfall variations in Southern Brazil from trace element ratios (Mg/Ca and Sr/Ca) in a Late Pleistocene stalagmite. Geochim. Cosmochim. Acta 71, 2250–2263.
Denton, G.H., Heusser, C.J., Lowell, T.V., Moreno, P.I., Andersen, B.G., Heusser, L.E., Schlfichter, C., Marchant, D.R., 1999. Interhemispheric linkage of paleoclimate during the last glaciation. Geogr. Ann. 81A, 107–153.
Farrera, I., Harrison, S.P., Prentice, I.C., Ramstein, G., Guiot, J., Bartlein, P.J., Bonnefille, R., Bush, M., Cramer, W., von Grafenstein, U., Holmgren, K., Hooghiemstra, H., Hope, G., Jolly, D., Lauritzen, S.-E., Ono, Y., Pinot, S., Stute, M., Yu, G., 1999. Tropical climates at the last glacial maximum: a new synthesis of terrestrial palaeoclimate data. I. Vegetation, lake-levels and geochemistry. Clim. Dyn. 15, 823–856.
Fontana, S.L., Bennett, K.D., 2012. Postglacial vegetation dynamics of western Tierra del Fuego. Holocene 22, 1337–1350.
Frumento, O., 2000. The severe precipitation event of April 1998 in north-east Patagonia. In: Preprints, Sixth Int. Conf. On Southern Hemisphere Meteorology and Oceanography, Boulder, CO. Amer. Meteor. Soc. 406–407.
Galloway, R.W., Markgraf, V., Bradbury, P., 1988. Dating shorelines of lakes in Patagonia, Argentina. J. South Am. Earth Sci. 1, 195–198.
Garreaud, R.D., Vuille, M., Compagnucci, R., Marengo, J., 2009. Present-day south american climate. Palaeogeogr. Palaeoclimatol. Palaeoecol. 281, 180–195.
Heine, K., 2000. Tropical South America during the Last Glacial Maximum: evidence from glacial, periglacial and fluvial records. Quat. Int. 72, 7–21.
Heusser, C.J., Heusser, L.E., Lowell, T.V., 1999. Paleoecology of the southern Chilean Lake District - Isla Grande de Chiloé during middle-late Llanquihue glaciation and deglaciation. Geogr. Ann. 81A, 231–284.
Heusser, C.J., Lowell, T.V., Heusser, L.E., Moreira, A., Moreira, S., 2000. Pollen sequence from the Chilean lake district during the Llanquihue glaciation in marine oxygen isotope stages 4–2. J. Quat. Sci. 15, 115–125.
Heusser, C.J., 2003. Ice Age Southern Andes: A Chronicle of Palaeoecological Events. Elsevier, Netherlands.
Heusser, L., Heusser, C.J., Mix, A., McManus, J., 2006. Chilean and Southeast Pacific paleoclimate variations during the last glacial cycle: directly correlated pollen and d18O records from ODP Site 1234. Quat. Sci. Rev. 25, 3404–3415.
Hoffman, J., 1975. Maps of Mean Temperature and Precipitation. Climatic Atlas of South America. WMO/UNESCO, Geneva.
Hughes, P.D., Gibbard, P.L., 2015. A stratigraphical basis for the last glacial maximum (LGM). Quat. Int. 383, 174–185.
Hulton, N.R.J., Purves, R.S., McCulloch, R.D., Sugden, D.E., Bentley, M.J., 2002. The last glacial maximum and deglaciation in southern South America. Quat. Sci. Rev. 21, 233–241.
Kageyama, M., Braconnot, P., Bopp, L., Mariotti, V., Roy, T., Woillez, M.-N., Caubel, A., Foujols, M.-A., Guilyardi, E., Khodri, M., Lloyd, J., Lombard, F., Marti, O., 2013. Mid-Holocene and Last Glacial Maximum climate simulations with the IPSL model. Part II: model-data comparisons. Clim. Dyn. 40, 2469–2495.
Kalnay, E., Kanamitsu, M., Kistler, R., Collins, W., Deaven, D., Gandin, L., Iredell, M., Saha, S., White, G., Woollen, J., Zhu, Y., Leetmaa, A., Reynolds, R., Chelliah, M., Ebisuzaki, W., Higgins, W., Janowiak, J., Mo, K.C., Ropelewski, C., Wang, J., Jenne, R., Joseph, D., 1996. The NCEP/NCAR 40-year reanalysis project. Bull. Am. Meteor. Soc. 77, 437–471.
Khodri, M., Kageyama, M., Roche, D.M., 2009. Sensitivity of South American tropical climate to Last Glacial Maximum boundary conditions: focus on teleconnections with tropics and extratropics. In: Vimeux, F., Sylvestre, F., Khodri, M. (Eds.), Past Climate Variability in South America and Surrounding Regions. Springer, pp. 213–238.
Kim, S.-J., Crowley, T.J., Erickson, D.J., Govindasamy, B., Duffy, P.B., Yong Lee, B., 2008. High-resolution climate simulation of the last glacial maximum. Clim. Dyn. 31, 1–16.
Kliem, P., Buylaert, J.P., Hahn, A., Mayr, C., Murray, A., Ohlendorf, C., Wastegård, S., Veres, D., Zolitschka, B., the PASADO Science Team, 2013. Magnitude, geomorphologic response and climate links of lake-level oscillations at Laguna Potrok Aike, Patagonian steppe (Argentina). Quat. Sci. Rev. 71, 131–146.
Kohfeld, K., Graham, R., de Boer, A., Sime, L., Wolff, E., Le Quéré, C., Bopp, L., 2013. Southern hemisphere westerly wind changes during the Last Glacial Maximum: paleodata synthesis. Quat. Sci. Rev. 68, 76–95.
Lamy, F., Hebbeln, D., Wefer, G., 1999. High-resolution marine record of climatic change in mid-latitude Chile during the last 28,000 years based on terrigenous sediment parameters. Quat. Res. 51, 83–93.
Lamy, F., Kaiser, J., Ninnemann, U., Hebbeln, D., Arz, H., Stoner, J., 2004. Antarctic timing of surface water changes off Chile and Patagonian Ice Sheet response. Science 304, 1959–1962.
Maldonado, A., Betancourt, J.L., Latorre, C., Villagrán, C., 2005. Pollen analyses from a 50000-yr rodent midden series in the southern Atacama Desert (25°30'S). J. Quat. Sci. 20, 493–507.
Marchant, R., Cleef, A., Harrison, S.P., Hooghiemstra, H., Markgraf, V., van Boxel, J., Ager, T., Almeida, L., Anderson, R., Baied, C., Behling, H., Berrio, J.C., Burbridge, R., Bjorck, S., Byrne, R., Bush, M., Duivenvoorden, J., Flenley, J., De Oliveira, P., van Geel, B., Graf, K., Gosling, W.D., Harbele, S., van der Hammen, T., Hansen, B., Horn, S., Kuhry, P., Ledru, M.-P., Mayle, F., Leyden, B., Lozano-García, S., Melief, A.M., Moreno, P., Moar, N.T., Prieto, A., van Reenen, G., Salgado-Labouriau, M., Schabitz, F., Schreve-Brinkman, E.J., Wille, M., 2009. Pollen-based biome reconstructions for Latin America at 0, 6000 and 18000 radiocarbon years ago. Clim. Past. 5, 725–767.
Markgraf, V., Dodson, J.R., Kershaw, P.A., McGlone, M., Nicholls, N., 1992. Evolution of late Pleistocene and Holocene climates in circum South Pacific land areas. Clim. Dyn. 6, 193–211.
Markgraf, V., Huber, U.M., 2010. Late and postglacial vegetation and fire history in Southern Patagonia and Tierra del Fuego. Palaeogeogr. Palaeoclimatol. Palaeoecol. 297, 351–366.
Massaferro, J., Larocque-Tobler, I., Brooks, S.J., Vandergoes, M., Dieffenbacher-Krall, A., Moreno, P., 2014. Quantifying climate change in Huelmo mire (Chile, Northwestern Patagonia) during the Last Glacial Termination using a newly developed chironomid-based temperature model. Palaeogeogr. Palaeoclimatol. Palaeoecol. 399, 214–224.
Mayle, F., Burn, M., Power, M., Urrego, D., 2009. Vegetation and fire at the Last Glacial Maximum in tropical South America. In: Vimeux, F., Sylvestre, F., Khodri, M. (Eds.), Past Climate Variability in South America and Surrounding Regions. Springer, pp. 89–112.
Mayr, Ch, Wille, M., Haberzettl, T., Fey, M., Janssen, S., Lucke, A., Ohlendorf, Ch, Oliva, G., Schabitz, F., Schleser, G., Zolitschka, B., 2007. Holocene variability of the southern hemisphere westerlies in argentinean Patagonia (52°S). Quat. Sci. Rev. 26, 579–584.
McCormac, F.G., Hogg, A.G., Blackwell, P.G., Buck, C.E., Higham, T.F.G., Reimer, P.J., 2004. SHCal04 southern hemisphere calibration 0–1000 cal BP. Radiocarbon 46, 1087–1092.

Mix, A.C., Bard, E., Schneider, R., 2001. Environmental processes of the ice age: land, oceans, glaciers (EPILOG). Quat. Sci. Rev. 20, 627–657.
Moreno, P.I., 1997. Vegetation and climate near Lago Llanquihue in the Chilean lake district between 20200 and 9500 14C yr BP. J. Quat. Sci. 12, 485–500.
Moreno, P.I., Denton, G.H., Moreno, H., Lowell, T.V., Putnam, A.E., Kaplan, M.R., 2015. Radiocarbon chronology of the last glacial maximum and its termination in northwestern Patagonia. Quat. Sci. Rev. 122, 233–249.
Niebler, H.-S., Arz, H.W., Donner, B., Mulitza, S., Patzold, J., Wefer, G., 2003. Sea surface temperatures in the equatorial and south Atlantic Ocean during the Last Glacial Maximum (23–19 ka). Paleoceanography 18 (3), 1069. http://dx.doi.org/10.1029/2003PA000902.
Otto-Bliesner, B., Brady, E., Clauzet, G., Tomas, R., Levis, S., Kothavala, Z., 2006. Last Glacial Maximum and holocene climate in CCSM3. J. Clim. 19, 2526–2544.
Paduano, G.M., Bush, M.B., Baker, P.A., Fritz, S.C., Seltzer, G.O., 2003. A vegetation and fire history of Lake Titicaca since the Last Glacial Maximum. Palaeogeogr. Palaeoclimatol. Palaeoecol. 194 (1–3), 259–279.
Ponce, F., Rabassa, J., Coronato, A., Borromei, A., 2011. Paleogeographic evolution of the atlantic coast of Pampa and Patagonia since the Last Glacial Maximum to the middle holocene. Biol. J. Linn. Soc. 103, 363–379.
Ponce, J.F., Fernández, M., 2014. Climatic and Environmental History of Isla de los Estados. Springer, Argentina.
Prohaska, F., 1976. The climate of Argentina, Paraguay and Uruguay. In: Schwerdtfeger, W. (Ed.), Climates of Central and South America, World Survey of Climatology. Elsevier, pp. 13–72.
Rabassa, J., Clapperton, C.M., 1990. Quaternary glaciations of the southern Andes. Quat. Sci. Rev. 9, 153–174.
Rojas, M., Moreno, P.I., Kageyama, M., Crucifix, M., Hewitt, Ch, Abe-Ouchi, A., Ohgaito, R., Brady, E.C., Hope, P., 2009. The Southern Westerlies during the last glacial maximum in PMIP2 simulations. Clim. Dyn. 32, 525–548.
Rojas, M., 2013. Sensitivity of southern hemisphere circulation to LGM and 4xCO2 climates. Geophys. Res. Lett. 40 http://dx.doi.org/10.1002/grl.50195.
Sagredo, E.A., Moreno, P.I., Kaplan, M.R., Villa-Martínez, R.P., 2011. Fluctuations of the Última Esperanza ice Lobe (52°S), Chilean Patagonia, during the last glacial maximum and termination 1. Geomorphology 125 (1), 92–108.
Saia, S., Pessenda, L., Gouveia, S., Aravena, R., Bendassolli, J., 2008. Last glacial maximum (LGM) vegetation changes in the Atlantic Forest, southeastern Brazil. Quat. Int. 184 (1), 195–201.
Satyamurti, P., Nobre, C., Silva Dias, P., 1998. South America. In: Karoly, D., Vincent, G. (Eds.), Meteorology of the Southern Hemisphere. American Meteorological Society, Boston, pp. 119–139.
Silvestri, G., Vera, C., Jacob, D., Pfeifer, S., Teichmann, C., 2009. A high-resolution 43-year atmospheric hindcast for South America generated with the MPI regional model. Clim. Dyn. 32, 693–709.
Sime, L.C., Kohfeld, K.E., Le Quéré, C., Wolff, E.W., de Boer, A.M., Graham, R.M., Bopp, L., 2013. Southern Hemisphere westerly wind changes during the Last Glacial Maximum: model-data comparison. Quat. Sci. Rev. 64, 104–120.
Solman, S.A., Sanchez, E., Samuelsson, P., da Rocha, R., Li, L., Marengo, J., Pessacg, N., Remedio, A., Chou, S.C., Berbery, H.E., Treut, H.L., de Castro, M., Jacob, D., 2013. Evaluation of an ensemble of regional climate model simulations over South America driven by the ERA-Interim reanalysis: models' performance and uncertainties. Clim. Dyn. 41, 1139–1157.
Stuiver, M., Reimer, P.J., Reimer, R.W., 2005. Calib 5.0.1. http://calib.qub.ac.uk/calib/.
Sylvestre, F., 2002. A high resolution diatom-reconstruction between 21,000 and 17,000 ^{14}C yr BP from the southern Bolivian Altiplano (18-23°S). J. Paleolimnol. 27, 45–57.
Sylvestre, F., 2009. Moisture pattern during the last glacial maximum in south America. In: Vimeux, F., Sylvestre, F., Khodri, M. (Eds.), Past Climate Variability in South America and Surrounding Regions. Springer, pp. 3–28.
Tammone, M.N., Hajduk, A., Arias, P., Teta, P., Lacey, E.A., Pardiñas, U.F.J., 2014. Last glacial maximum environments in northwestern Patagonia revealed by fossil small mammals. Quat. Res. 82 (1), 198–208.
Taylor, K., Stouffer, R., Meehl, G., 2012. An overview of CMIP5 and the experiment design. Bull. Am. Meteor. Soc. 93, 485–498.
Tonni, E.P., Cione, A.L., Figini, A.J., 1999. Predominance of arid climates indicated by mammals in the pampas of Argentina during the late Pleistocene and Holocene. Palaeogeogr. Palaeoclimatol. Palaeoecol. 147, 257–281.
Valdes, P.J., 2000. South American palaeoclimate model simulations: how reliable are the models? J. Quat. Sci. 15 (4), 357–368.
Vera, C., Silvestri, G., Liebmann, B., González, P., 2006. Climate change scenarios for seasonal precipitation in South America from IPCC-AR4 models. Geophys. Res. Lett. 33, L13707. http://dx.doi.org/10.1029/2006GL025759.
Villagrán, C., 1990. Glacial climates and their effects on the history of the vegetation of Chile: a synthesis based on palynological evidence from Isla de Chiloé. Rev. Palaeobot. Palynol. 65, 17–24.
Vizy, E.K., Cook, K.H., 2005. Evaluation of Last Glacial Maximum sea surface temperature reconstructions through their influence on South American climate. J. Geophys. Res. 110, D11105. http://dx.doi.org/10.1029/2004JD005415.
Wainer, I., Clauzet, G., Ledru, M.-P., Brady, E., Otto-Bliesner, B., 2005. Last glacial maximum in south America: paleoclimate proxies and model results. Geophys. Res. Lett. 32, L08702. http://dx.doi.org/10.1029/2004GL021244.
Wang, X., Auler, A.S., Edwards, R.L., Cheng, H., Ito, E., Wang, Y., Kong, X., Solheid, M., 2007. Millennial-scale precipitation changes in southern Brazil over the past 90,000 years. Geophys. Res. Lett. 34, L23701. http://dx.doi.org/10.1029/2007GL031149.
Whitney, B.S., Mayle, F.E., Punyasena, S.W., Fitzpatrick, K.A., Burn, M.J., Guillen, R., Chavez, E., Mann, D., Pennington, R.T., Metcalfe, S.E., 2011. A 45 kyr palaeoclimate record from the lowland interior of tropical South America. Palaeogeogr. Palaeoclim. Palaeoecol. 307, 177–192.
Wilks, D.S., 2006. Statistical Methods in the Atmospheric Sciences, second ed. International Geophysics Series. Elsevier Academic Press, St. Louis.
Xie, P., Arkin, P., 1997. Global precipitation: a 17-year monthly analysis based on gauge observations, satellite estimates, and numerical model outputs. Bull. Amer. Meteor. Soc. 78, 2539–2558.
Zolitschka, B., Anselmetti, F., Ariztegui, D., Corbella, H., Francus, P., Lücke, A., Maidana, N.I., Ohlendorf, C., Schäbitz, F., Wastegård, S., 2013. Environment and climate of the last 51,000 years - new insights from the Potrok Aike maar lake sediment archive drilling project (PASADO). Quat. Sci. Rev. 71, 1–12.